Geological Society, London, Special Publications Online First

Are terrestrial plumes from motionless plates analogues to Martian plumes feeding the giant shield volcanoes?

Christine M. Meyzen, Matteo Massironi, Riccardo Pozzobon and Luca Dal Zilio

Geological Society, London, Special Publications, first published February 21, 2014; doi 10.1144/SP401.8

Notes

Are terrestrial plumes from motionless plates analogues to Martian plumes feeding the giant shield volcanoes?

CHRISTINE M. MEYZEN[1]*, MATTEO MASSIRONI[1,2], RICCARDO POZZOBON[1,3] & LUCA DAL ZILIO[1]

[1]*Dipartimento di Geoscienze, Università degli Studi di Padova, via G. Gradenigo, 6, 35131 Padova, Italy*

[2]*INAF, Osservatorio Astronomico di Padova, Vicolo dell'Osservatorio 3, 35122 Padova, Italy*

[3]*IRSPS-DISPUTer, Universita' G. d'Annunzio, Via Vestini 31, 66013 Chieti, Italy*

**Corresponding author (e-mail: christine.meyzen@unipd.it)*

Abstract: On Earth, most tectonic plates are regenerated and recycled through convection. However, the Nubian and Antarctic plates could be considered as poorly mobile surfaces of various thicknesses that are acting as conductive lids on top of Earth's deeper convective system. Here, volcanoes do not show any linear age progression, at least not for the last 30 myr, but constitute the sites of persistent, focused, long-term magmatic activity rather than a chain of volcanoes, as observed in fast-moving plate plume environments. The melt products vertically accrete into huge accumulations. The residual depleted roots left behind by melting processes cannot be dragged away from the melting loci underlying the volcanoes, which may contribute to producing an unusually shallow depth of oceanic swells. The persistence of a stationary thick depleted lid slows down the efficiency of melting processes at shallow depths. Numerous characteristics of these volcanoes located on motionless plates may be shared by those of the giant volcanoes of the Tharsis province, as Mars is a one-plate planet. The aim of this chapter is to undertake a first inventory of these common features, in order to improve our knowledge of the construction processes of Martian volcanoes.

The near-'one-plate planet' evolutionary history of Mars has led to the formation of its long-lasting giant shield volcanoes, which dominate the topography of its western hemisphere. Unlike Earth, Mars would have been a transient convecting planet, where plate tectonics would have possibly acted only during the first few hundreds of millions of years of its history (e.g. Sleep 1994; Bouvier *et al.* 2009). Most Martian magmatic activity is probably very old (Noachian) and has been preserved in the near-absence of crustal recycling, in contrast to Earth (Phillips *et al.* 2001; Taylor *et al.* 2006; Werner 2009; Carr & Head 2010). Recent volcanic resurgence occurred in the main Martian volcanic provinces, Tharsis (Fig. 1) and Elysium, during the Amazonian Period (Werner 2009).

Although the large igneous provinces of Mars bear some geomorphological similarities with terrestrial oceanic plateaus, they distinguish themself by their larger scales. Martian volcano heights commonly reach three times those of Hawaiian volcanoes (Plescia 2004; Carr 2006), while they are generally many hundreds of kilometres in breadth. Their accretion, which is vertical due to the absence of lateral plate movement and crustal recycling, loads the lithosphere, and causes lithospheric flexure, deformation and edifice flank compressional failure (e.g. McGovern & Solomon 1993; Phillips *et al.* 2001; McGovern *et al.* 2002; McGovern & Morgan 2009; Byrne *et al.* 2013). Underlying these huge volcanoes, the lithosphere might reach a thickness of up to 150 km to provide isostatic support (Zuber *et al.* 2000; McGovern *et al.* 2002). Thickening of the lithosphere (17–25 km Ga^{-1}) occurs over time as a result of decreasing mantle potential temperature (30–40 K Ga^{-1}) (Baratoux *et al.* 2011). This thickening of the lithospheric lid increases the final depth of melting and thereby reduces the mean degree of melting. Such a process leads to less efficient melt extraction and subsequent mixing, favouring mantle–melt interaction and high-pressure melt fractionation. Such lithospheric processes are commonly observed in near-stationary plate plume settings (velocity <25 mm a^{-1}).

We note, however, that while Hawaiian islands are located on a fast-moving plate (i.e. the Pacific plate, 65 mm a^{-1}: Argus *et al.* 2011), Hawaiian hotspot intraplate magmatic activity has commonly been considered as some of the best analogues to that observed on Mars (e.g. Zuber & Mougins-Mark 1992; McGovern & Solomon 1993; Plescia 2004; Carr 2006; Bleacher *et al.* 2007; Byrne *et al.* 2013). However, intraplate oceanic volcanism of

From: Platz, T., Massironi, M., Byrne, P. K. & Hiesinger, H. (eds) *Volcanism and Tectonism Across the Inner Solar System*. Geological Society, London, Special Publications, **401**, http://dx.doi.org/10.1144/SP401.8

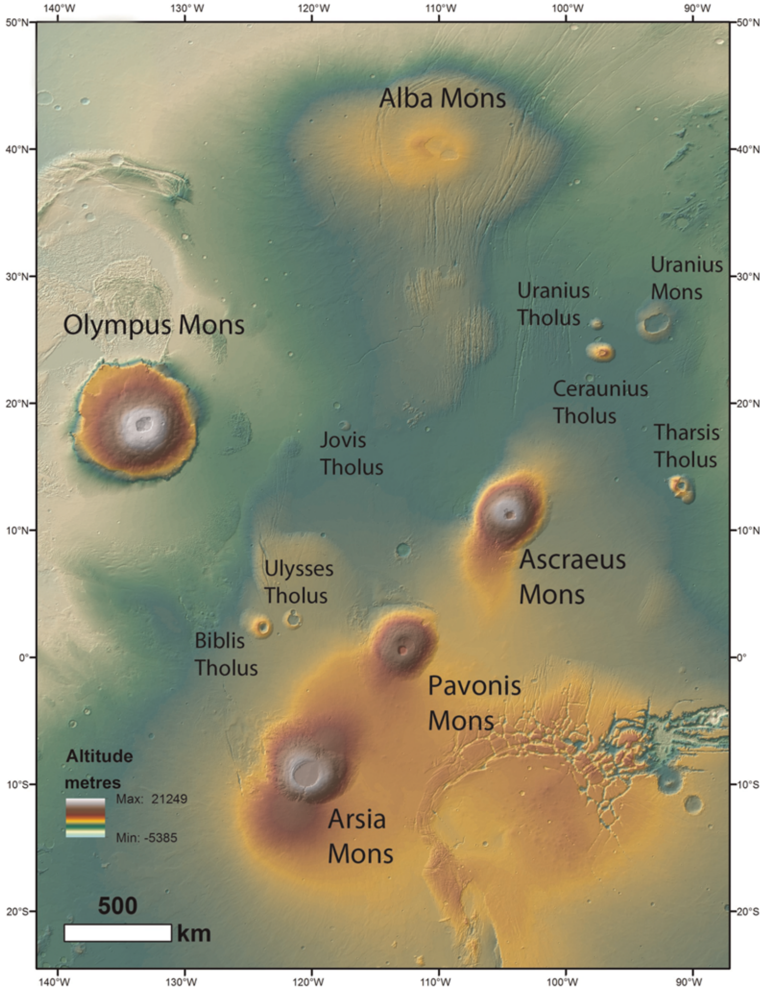

Fig. 1. Topographical map of the Tharsis province produced from Mars Orbiter Laser Altimeter (MOLA) data, with the labels showing the location of major volcanic edifices.

slow-moving plates such as the Crozet or Cape Verde islands might represent a better analogue. As on Mars, volcanoes at slow-moving plates do not show any linear age progression, but constitute the sites of persistent, long-term magmatic activity. Because the lithosphere lid is near-stagnant in these areas, the melting mantle region concentrates its products in a single area rather than them being spread out, as observed in fast-moving plate plume environments such as the Hawaiian–Emperor seamount chain on the Pacific seafloor. The melt products vertically accrete into huge accumulations, and oceanic swell heights are unusually shallow for their ages (Fig. 2). Processes of thermal reheating and mechanical weakening of the lithosphere might also be enhanced. The loading of the lithosphere by the volcanic accumulations might ultimately cause edifice collapse and/or flexural deformation. These processes are probably similar to those observed on Mars.

The goal of this paper is to describe the essential characteristics of intra-oceanic plumes on slow-moving plates on Earth and to compare them to large shield volcanoes in the Tharsis region of Mars. Specific similarities will be described, whereas some peculiar features, either compositional or morphological and common among these terrestrial volcanoes but not yet detected on Mars, will be emphasized as main objectives for future research. Speculations on deep processes that could have controlled the construction and development of large shield volcanoes on Mars are also

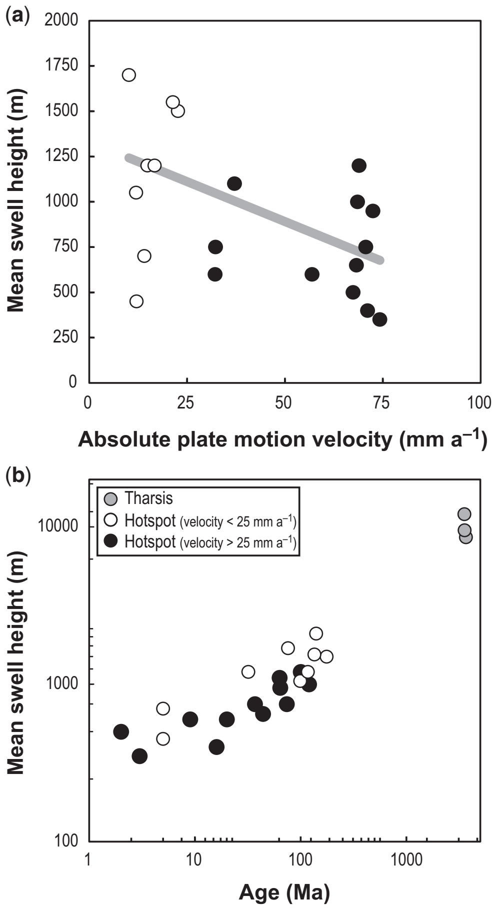

Fig. 2. (**a**) Mean swell height (m) as a function of absolute plate motion velocity (mm a^{-1}) for 21 oceanic islands. The velocities were calculated with the NNR-MORVEL56 model of Argus *et al.* (2011). Filled dots denote locations with plate velocities of >25 mm a^{-1}, while open dots denote those of <25 mm a^{-1}. The mean swell heights are from Monnereau & Cazenave (1990). (**b**) Mean swell height (m) as a function of the age of oceanic lithosphere (Ma). Mean swell heights and ages are from Monnereau & Cazenave (1990). The mean swell height for Tharsis was calculated from Mars Orbiter Laser Altimeter (MOLA) data, as described in Figure 9.

made on the basis of what is known and soundly hypothesized for plumes located on slow-moving oceanic plates.

The Tharsis magmatic province

The Tharsis volcanic province is one of the most noticeable global-scale physiographical feature on Mars, covering about 20% of its surface area in the western hemisphere (Fig. 1). Its areal extent (>6.5×10^6 km^2) is far greater than that of the largest terrestrial igneous provinces. This magmatic province is located near the boundary of the Martian crustal dichotomy between the northern lowland and the southern uplands. It extends from the northern lowland plains southwards to Solis Planum, and from Arcadia Planitia eastwards to Lunae Planum. Its topography describes a bulge-like structure, above which rest massive shield volcanoes (e.g. >500 km wide and up to 25 km high: Fig. 1). Both effusive lava flows and pyroclastic activity have built up these edifices (e.g. Wilson & Head 1994).

These large shield volcanoes, such as Olympus Mons, may have been emplaced on very thick elastic lithosphere (T_e of more than 100 km) (Zuber *et al.* 2000; McGovern *et al.* 2002; Grott *et al.* 2013), meaning that the Tharsis region overlies some of the thickest lithosphere of Mars. But lithospheric thicknesses of less than 50 km also support a few volcanoes in the Tharsis region (Grott & Breuer 2009; Grott *et al.* 2013). Their crustal thickness is highly variable at a regional scale (Zuber *et al.* 2000). The old Alba Patera volcano (3.02 Ga: Robbins *et al.* 2011) is underlain by thick crust, whereas the region beneath the younger shields such as Olympus and Tharsis Montes (Arsia, Pavonis and Ascraeus) would have experienced apparent crustal thinning (Zuber *et al.* 2000). The major volcanic loading exerted by Tharsis volcanoes, with concomitant effects on deformation of the Martian lithosphere that is mirrored by a broad free-air anomaly, would help define the present-day long-wavelength gravity field of Mars (Phillips *et al.* 2001; Golle *et al.* 2012).

The gravity, topography and tectonic attributes of this region have been ascribed to one or more of the following processes: (1) a large-scale mantle convective upwelling (e.g. Schubert *et al.* 1990; Zhong & Zuber 2001; Roberts & Zhong 2006; Keller & Tackley 2009), inducing dynamic topography; (2) regional uplift due to lateral migration and intrusion of material thermally eroded from the base of the crust of the lowlands (Wise *et al.* 1979) or due to massive intrusion (i.e. 85% of the total magmatic products; Phillips *et al.* 1990) in the crust and upper mantle; (3) flexural loading from volcanic construction (Solomon & Head 1982; Phillips *et al.* 2001), possibly compensated by a depleted root (Finnerty *et al.* 1988); (4) preferential concentration of volcanism along early impact-basin ring structures (Schultz *et al.* 1982); and (5) edge-driven convection (King & Redmond 2005).

Among these processes, the first appears to be the main building mechanism for the Tharsis province through time. The formation of large-scale mantle plumes may be driven by viscosity layering in the mid-mantle (Zhong & Zuber 2001; Roberts & Zhong 2006), an endothermic phase change near the core–mantle boundary (Zhong 2009; Šrámek & Zhong 2012) or an early impact-induced thermal anomaly (Golabek *et al.* 2011). Large-scale upwelling driven by degree-1 mantle convection (i.e. whereby one hemisphere is dominated by an upwelling, while the other encompasses a downwelling), which is induced by layered mantle viscosity, is predicted to be short lived with a timescale development ranging from 1 to several hundred million years (myr) (Zhong & Zuber 2001; Roberts & Zhong 2006). These large-scale upwellings would tend to migrate towards regions of lower lithospheric thickness, which can account for the location of the Tharsis province at the dichotomy boundary (Zhong 2009; Šrámek & Zhong 2012). Convection driven by endothermic phase transition near the core–mantle boundary may also promote the formation and focusing of long-lived plumes at Tharsis, as well as late-stage volcanism (Harder 2000; Grott *et al.* 2013). In this case, the development of a degree-1 pattern would require at least 5 billion years (Wenzel *et al.* 2004; Roberts & Zhong 2006), but recent three-dimensional (3D) convection models with temperature-dependent rheology instead require a shorter formation timescale (Buske 2006). Another potential mechanism for stabilizing long-lived plumes at Tharsis is provided by a thick, low-density depleted mantle layer with non-linear conductivity (Schott *et al.* 2001), where minima in thermal conductivity values promote the reoccurrence of thermal instabilities. However, such a model fails to predict the generation of the Tharsis province at the dichotomy boundary (Grott *et al.* 2013). Excess mantle heat arising from an early giant impact, which would have first created the southern highlands crust, might also have triggered the formation of a transient superplume underneath the impacted hemisphere, inducing massive volcanism at Tharsis (Golabek *et al.* 2011). After more than 100 myr, the impact-induced plume is predicted to slowly regress, while new upwellings would form throughout the mantle (Golabek *et al.* 2011).

Most magmatic activity in the Tharsis region is Noachian (>3.7 Ga) in age, but the large shield volcanoes continued to grow up to the Amazonian (<3 Ga) to a lesser degree (Hartman & Neukum 2001; Werner 2009). In particular, the average eruption rate would have dropped from approximately 0.04 $km^3\ a^{-1}$ in the Noachian and Hesperian to approximately 0.01 $km^3\ a^{-1}$ in the Amazonian (Greeley & Schneid 1991). Hence, Tharsis volcanoes were probably built up by eruptions widely spaced over a large timespan (Fig. 3). The clustering

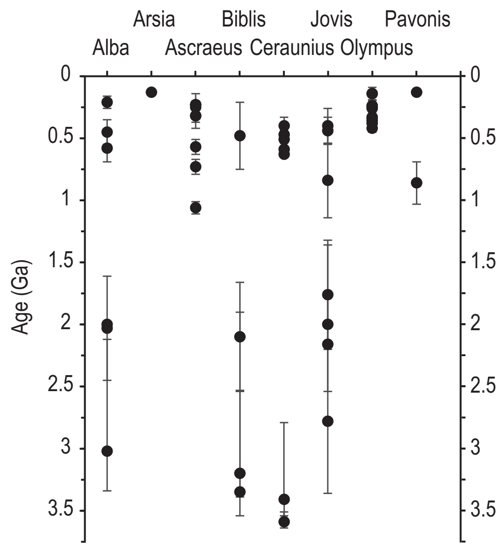

Fig. 3. Age distribution (Ga) of exposed calderas across the Tharsis province. Data are from Robbins *et al.* (2011).

of ages defined by lava flows and caldera floors (Neukum *et al.* 2004; Werner 2009; Robbins *et al.* 2011) confirms that magma supply was highly episodic (Fig. 3). The large shield volcanoes were characterized by very active periods with high effusion rates (as indicated by the large volume of many lava flows), separated by long periods of quiescence (e.g. Hiesinger *et al.* 2007; Giacomini *et al.* 2009; Hauber *et al.* 2011). During the Amazonian, a focusing of volcanism has been recorded between 1.6 and 1 Ga (Werner 2009), whereas the most recently erupted lava flows and the last caldera collapses are, indeed, very young (200–100 Ma) (Neukum *et al.* 2004; Werner 2009; Robbins *et al.* 2011; Pozzobon *et al.* 2014).

Shallow magma plumbing architectures fed by dykes probably constructed the major volcanic edifices of Tharsis (Wilson & Head 1994). Early estimates of magma chamber depths in Tharsis shields range between 9 and 16 km below the summit (Zuber & Mouginis-Mark 1992; Wilson & Head 1998). However, a recent study of Ascreaus Mons suggests a two-level architecture of the underground magma plumbing system, with some fractionation of magmas occurring within the uppermost mantle (Pozzobon *et al.* 2014). In addition, some of the nested calderas on the Tharsis Montes imply the existence of several shallow and large magma reservoirs, which are thermally viable for only a limited period of time (Wilson *et al.* 2001). The morphology of some late-stage lavas erupted near Jovis Tholus also suggests short-duration crustal storage (Wilson *et al.* 2009). Other evidence for multiple stages of magma ascent and withdrawal are provided by the complex geometry of summit calderas at Olympus and Ascraeus Montes (Mouginis-Mark & Robinson 1992; Crumpler *et al.* 1996; Scott & Wilson 2000; Byrne *et al.* 2012).

Average surface heat flux values for individual Tharsis volcanoes derived from the effective elastic thickness since the time of loading range from 14 to 35 mW m^{-2} (McGovern *et al.* 2002). When considering the superficial distribution of heat-producing elements, other estimates of heat fluxes encompass this range and show a similar geographical pattern, with gradually increasing values from 22 to 24 mW m^{-2} in the north to more than 26 mW m^{-2} in the south, along the Tharsis Montes (Grott & Breuer 2010). It is interesting to note that Olympus Mons exhibits the smallest heat flux of the volcanoes from the Tharsis province (McGovern *et al.* 2002; Grott *et al.* 2013). However, when hot mantle upwelling underneath these regions is taken into consideration, these local heat flow values are predicted to be at least twice as great (Grott & Breuer 2010; Grott *et al.* 2013).

At the planetary scale, recent comprehensive geochemical mapping of the Tharsis region by gamma ray spectrometer (GRS: Boynton *et al.* 2007; Newsom *et al.* 2007; El Maarry *et al.* 2009; Taylor *et al.* 2010; Baratoux *et al.* 2011) has shown that this region distinguishes itself in exhibiting some of the most depleted patterns in K, Th, Fe, Si and Ca among the geochemical composition spectrum exhibited by the six provinces of the Martian crust (Taylor *et al.* 2010). Although Si and Fe concentrations are depleted relative to those of other regions on Mars, they are lower and higher, respectively, than those of any terrestrial primary magma compositions (El Maarry *et al.* 2009). GRS chemical imaging reveals two distinct provinces (Boynton *et al.* 2007; El Maarry *et al.* 2009, Gasnault *et al.* 2010; Taylor *et al.* 2010; Baratoux *et al.* 2011), the boundary of which would lie to the north or south of Pavonis Mons. The Arsia, Pavonis and Olympus Montes have a lower Si, Th and Fe content than has Ascraeus (Fig. 4). Alba Mons is also distinct in that it exhibits the lowest Th, and some of the highest Fe, content of the Tharsis volcanoes (Fig. 4). The modelling of SiO_2–FeO systematics of these edifices shows that Ascraeus lavas can be produced by a slightly lower melting pressure (*c.* 1.6 GPa) and a higher degree of melting (*c.* 9%) than other Tharsis volcanoes (1.7–1.9 GPa, 5–8%). This implies the presence of a slightly higher mantle potential temperature underneath Ascraeus Mons (1384 °C) relative to other individual edifices from the Tharsis province (1340–1382 °C: Baratoux *et al.* 2011).

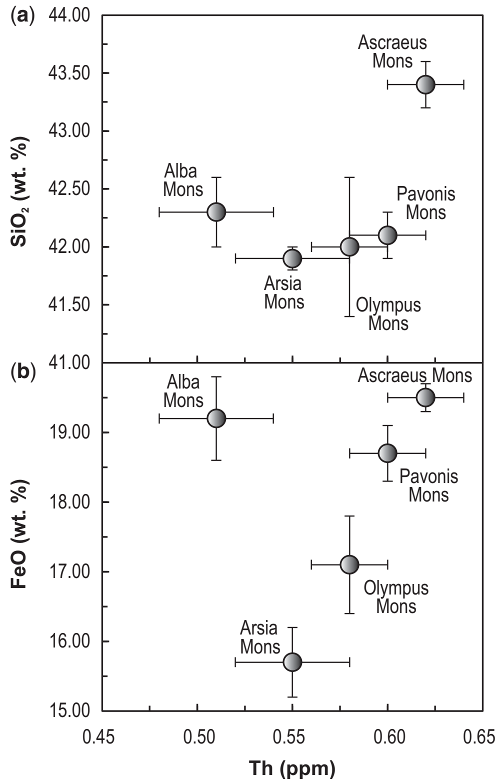

Fig. 4. Abundances of silica, thorium and iron oxide for five volcanoes from the Tharsis province: (**a**) SiO_2 v. Th; (**b**) FeO v. Th. Data are from Baratoux *et al.* (2011).

Terrestrial volcanoes at near-stagnant plates

On Earth, oceanic magmatism on a near-stagnant plate (less than 20 mm a^{-1}: Argus *et al.* 2011) is geographically restricted to the Antarctic plate, which has moved at an extremely slow velocity for the past 30 myr (15.2 mm a^{-1}: Argus *et al.* 2011) (Fig. 5). However, with the exception of the Kerguelen archipelago, very few data are available for most volcanoes emplaced on this plate (i.e. Bouvet, Marion and Crozet). We thus extend our study to volcanoes from the Nubian plate, which has an absolute motion of less than 25 mm a^{-1} according to Argus *et al.* 2011 (Fig. 5). This rate might be much lower, as another investigation suggests that the Nubian plate's absolute motion to the NE abruptly slowed at 30 Ma from 22 to about 10 mm a^{-1} (Silver *et al.* 1998). In addition, our interest includes volcanoes from archipelagos, for which geophysical and geochemical characteristics have been fully investigated (e.g. Canary, Madeira and Cape Verde). The emphasis will be placed

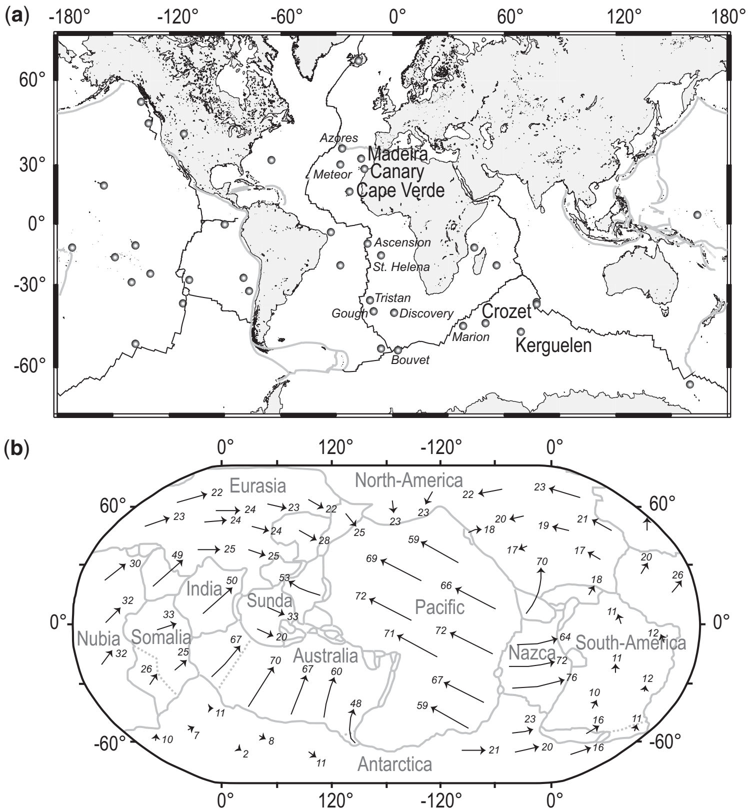

Fig. 5. (**a**) World map showing the distribution of prominent hotspots (modified from Lin 1998). (**b**) Plate map boundaries and their absolute horizontal velocities (mm a^{-1}, black arrows) in the NNR-MORVEL56 frame. Adapted and simplified from Argus *et al*. (2011).

mainly on those volcanoes atop an old and thick oceanic lithosphere (>50 Ma).

A near-stationary-lid regime, such as that of the Antarctic plate, should probably be much less efficient in transferring heat out of the planetary interior than a mobile-lid regime. The low buoyancy fluxes of some plumes located on slow-moving plates will further reinforce this effect. Plumes with less than 0.5 Mg s^{-1} (i.e. Crozet: Sleep 1990), if rising from the core–mantle boundary, should have cooled so much by heat diffusion that they would not melt beneath an old lithosphere (Albers & Christensen 1996). Weak plumes with a buoyancy flux of about 0.5 Mg s^{-1} have a 150 K or lower temperature anomaly in the upper mantle due to thermal diffusion (Steinberger & Antretter 2006). Therefore, such plumes may be sourced from shallower depths than the core–mantle boundary.

The majority of hotspots on slow-moving plates (i.e. less than 25 mm a^{-1}) exhibit topographical swell heights greater than those observed at faster plates for a given oceanic lithospheric age (Fig. 2) (Monnereau & Cazenave 1990). Sitting atop these swells, their islands in each archipelago often define a horseshoe-like shape (Cape Verde, Crozet and Canary for the last 30 myr). As the melting region remains geographically fixed with time, the melts are focused and seem to be pooled, forming huge accumulations. Consequently, the Azores, Cape Verde and Crozet bathymetric swells possess some of the greatest amplitudes among hotspot-influenced regions (Monnereau & Cazenave 1990) (Fig. 2). The scatter of gravity and bathymetric data for the Northern Kerguelen Plateau also provides evidence for a swell's signature (Sandwell & MacKenzie 1989; Wallace 2002). Other hotspots, such as those from the Canary and Madeira islands, appear to be associated with less substantial swell anomalies (Filmer & McNutt 1989; Monnereau & Cazenave 1990; Marks & Sandwell 1991; Canales & Danaobeitia 1998; Grevemeyer 1999; Ito & van Keken 2007) (Fig. 2) but with prominent geoid anomalies (Jung & Rabinowitz 1986; Cazenave *et al.* 1988). However, in the Canary Islands, as shown by seismic data, a thick sedimentary cover masks the buried moat (Watts *et al.* 1997; Canales & Danaobeitia 1998).

The building and evolution modes of bathymetric swells have essentially been modelled in Hawaii, and have been ascribed to one or more of the following processes: (1) thermal rejuvenation (e.g. Detrick & Crough 1978), whereby the oceanic lithosphere is heated as it passes over the hotspot and is therefore thinned, producing isostatic uplift of the swell; (2) dynamic pressure (e.g. Olson 1990; Sleep 1990), whereby the upwards buoyancy flux through the asthenosphere from the swell centre supports it; and (3) compositional and thermal buoyancy in a higher-viscosity depleted swell root (Morgan *et al.* 1995; Yamamoto *et al.* 2007). Upon melting, the dense minerals garnet and clinopyroxene in the residue are exhausted, leading to a decrease in Fe relative to Mg, which forms an intrinsically less dense depleted root and produces the swell uplift.

Morgan *et al.* (1995) ascribed the unusually shallow oceanic swells such as those of Cape Verde and Crozet (Fig. 2) to the persistence of a stationary, thick and depleted root, which has not been dragged away from the hotspot in the virtual absence of plate motion since 30 Ma. Indeed, evidence of the presence of low-velocity, low-density upper-mantle material at depths ranging from 40 to 81 km at Cape Verde, Canary, Kerguelen and Crozet islands are provided by deep seismic refraction and gravity data (Marks & Sandwell 1991; Recq & Charvis 1987; Charvis *et al.* 1995; Canales & Danaobeitia 1998; Lodge & Hellfrich 2006). These anomalies were interpreted by Morgan *et al.* (1995) to reflect the spreading, thinning and slight melting of a thick sublithospheric swell root.

However, the mechanisms that govern the generation and evolution of swells under a slow-moving plate have been investigated in detail in only a few localities. In the Cape Verde Islands, Lodge & Helffrich (2006), using seismic data to a depth of 120 km, highlighted the existence of low-density material with a non-radial flow distribution, spreading from separate melting loci under the swell. In the case of a dynamic pressure model, a flow field of homogeneous-viscosity material would emanate from the buoyancy flux centre with a radial anisotropic fabric. However, some investigators (Pim *et al.* 2008; Wilson *et al.* 2010) argue against the depleted root assumption, as no lateral variations in P-wave velocities are recorded in the upper 2 km of the mantle. Using measured heat flow, and geoid, seismic and bathymetric data, Wilson *et al.* (2010) have recently favoured dynamic upwelling (50–70%) as the main mechanism to sustain the swell, with minor contributions from thickened oceanic crust and partial thermal rejuvenation of the lithospheric mantle. We note that all studies of the Cape Verde Islands concluded that lithosphere reheating processes alone cannot account for the observed uplift (Courtney & White 1986; Ali *et al.* 2003; Lodge & Helffrich 2006; Pim *et al.* 2008). Several investigators at other locations (e.g. Liu & Chase 1989; Ribe & Christensen 1994) have also pointed out the inefficiency of thermomechanical erosion processes in sustaining a bathymetric swell. Even if endogenous growth of volcanoes is accompanied by intrusive accumulation of neutrally buoyant magma at the base of the crust, underplating also appears to play a minor role at best (although may be absent entirely) in elevating the seafloor (Grevemeyer 1999; Pim *et al.* 2008). In turn, seismic modelling does not show any evidence for underplating at the base of the crust (Pim *et al.* 2008). At the Crozet Islands, measured heat flow, geoid and bathymetric data suggest that the swell is dynamically supported, with a minor contribution coming from crustal thickening (Courtney & Recq 1986; Recq *et al.* 1998). Although the swell is masked by some sedimentary cover at the Canary Islands, Ye *et al.* (1999) identified underplating processes under Gran Canaria at depths of 17–26 km, with a thickness ranging from 8–10 km, but it is unclear whether thermal lithospheric rejuvenation played a role in its development (Canales & Danaobeitia 1998; Grevemeyer 1999). The weak swell observed at Madeira has been ascribed to reheating of the lower lithosphere (Sandwell & MacKenzie 1989; Grevemeyer 1999). At least for the archipelagos, for which the swells are well pronounced, dynamic pressure is favoured over thermal rejuvenation as the main mechanism to account for their formation. However, we caution that the role of a buoyant depleted swell root has been poorly investigated, although this mechanism may be far from negligible in such motionless environments.

For volcanoes emplaced on motionless plates, widely spaced heat-flow determinations have only been published for two oceanic swells: Crozet (96 mW m^{-2}: Courtney & Recq 1986) and Cape Verde (63 mW m^{-2}: Courtney & White 1986). These values are the only measurements of worldwide oceanic swells that are higher than the predicted values of reference models for the thermal evolution of oceanic lithosphere (Harris & McNutt 2007). If loss of heat by advection occurs, these values may underestimate the actual mantle flux (Harris & McNutt 2007). In addition, at low-degree melting environments, where a thick lithosphere lid is present, heat flow anomalies are less affected by the buffering effect of melting (Courtney & White 1986). When a rock melts, the latent heat of fusion consumes energy, inducing a temperature drop and causing a decrease in heat flow at the surface.

Wide-angle refraction seismic data for the Northern Kerguelen Plateau, Cape Verde, Crozet and the Canary Islands suggest the presence of a thickened crust for islands located on slow-moving plates ranging in thickness from 11–19 km (Banda *et al.* 1981; Recq & Charvis 1987; Recq *et al.* 1990, 1998; Charvis *et al.* 1995; Lodge & Helffrich 2006). At Tenerife, seismic and gravity data suggest that up to 1.5×10^5 km^3 of magmatic material has been added to the surface of the flexed oceanic crust that, assuming an age of 6–16 Ma for the shield-building stage on Tenerife, implies a magma generation rate of about 6×10^{-3}–2×10^{-2} km^3 a^{-1} (Watts *et al.* 1997). Using K–Ar ages, the average eruption rate for the entire Canary archipelago has been estimated at 6.8×10^{-3} km^3 a^{-1} by Hoernle & Schmincke (1993) (Fig. 6). Based on bathymetric, gravity and radiometric data, the mean magmatic rate at Cape Verde has been estimated at about 2×10^{-2}–2.6×10^{-2} km^3 a^{-1} (Fig. 6) (Morgan 1995; Holm *et al.* 2008). Madeira is characterized by some of the lowest eruption rates, ranging from 2×10^{-6} to 1.5×10^{-4} km^3 a^{-1}, with an average rate of 9.5×10^{-5} km^3 a^{-1} for the subaerial part of the shield stage at the Madeira and Desertas islands (Fig. 6) (Geldmacher *et al.* 2000). The rates determined for the Canary and Madeira islands are substantially lower than those calculated for the Hawaiian volcanoes (Fig. 6) (Bargar & Jackson 1974).

Although their eruption rates are among the lowest observed on Earth, the magmatic activity at least at the Canaries and Madeira islands distinguishes itself by its longevity, with volcanoes often remaining active for tens of millions of years (Fig. 7) (Carracedo 1999; Geldmacher *et al.* 2000, 2001). However, this activity is sporadic, with chronological gaps of up to 12 myr at Selvagen Islands (the Canary archipelago), periods of quiescence that are much longer than those observed in Hawaii (Fig. 7) (Geldmacher *et al.* 2001). Large time gaps also constitute a noteable feature of the Cape Verde Islands, where a period of 5 myr without activity has been documented at Maio (Fig. 7) (Holm *et al.* 2008).

Owing to high rates of subsidence, the individual islands of the Hawaiian archipelago have a relatively short lifespan. Most of the Hawaiian volcanoes have subsided by between 2 and 4 km since their emergence (Moore & Campbell 1987). The bulk of this subsidence occurred rapidly, probably within 1 myr of the end of the shield-building phase (Moore & Campbell 1987). In contrast, islands on motionless plates can be characterized by a near-absence of post-emergence subsidence, as observed at the Kerguelen, Cape Verde and Canary islands (Filmer & McNutt 1989; Carracedo 1999; Wallace 2002). Those islands of the Canary Islands older than 20 Ma are still emergent (e.g. Fuerteventura, at 25 Ma: Geldmacher *et al.* 2001), while islands in the Hawaiian–Emperor volcanic chain submerge by subsidence after about 7 myr (Fig. 7). All of these islands rest on a lithosphere older than that of Hawaii. As proposed by Funk & Schmincke (1998) for the Canary Islands, this stability may be due to a combination of minor recent volcanic loading and to a greater flexural rigidity of the old lithosphere beneath these islands. In addition, the compositional and thermal buoyancy

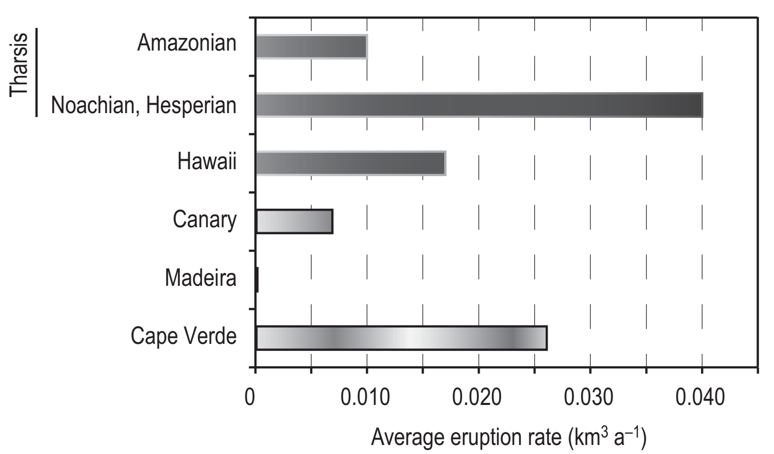

Fig. 6. Eruption rates (km^3 a^{-1}) from different oceanic islands and from the Tharsis province. Eruption rates for Hawaii, Canary, Madeira and Cape Verde are, respectively, from Bargar & Jackson (1974), Hoernle & Schmincke (1993), Geldmacher *et al.* (2000) and Holm *et al.* (2008). Those for the Tharsis province are from Greeley & Schneid (1991).

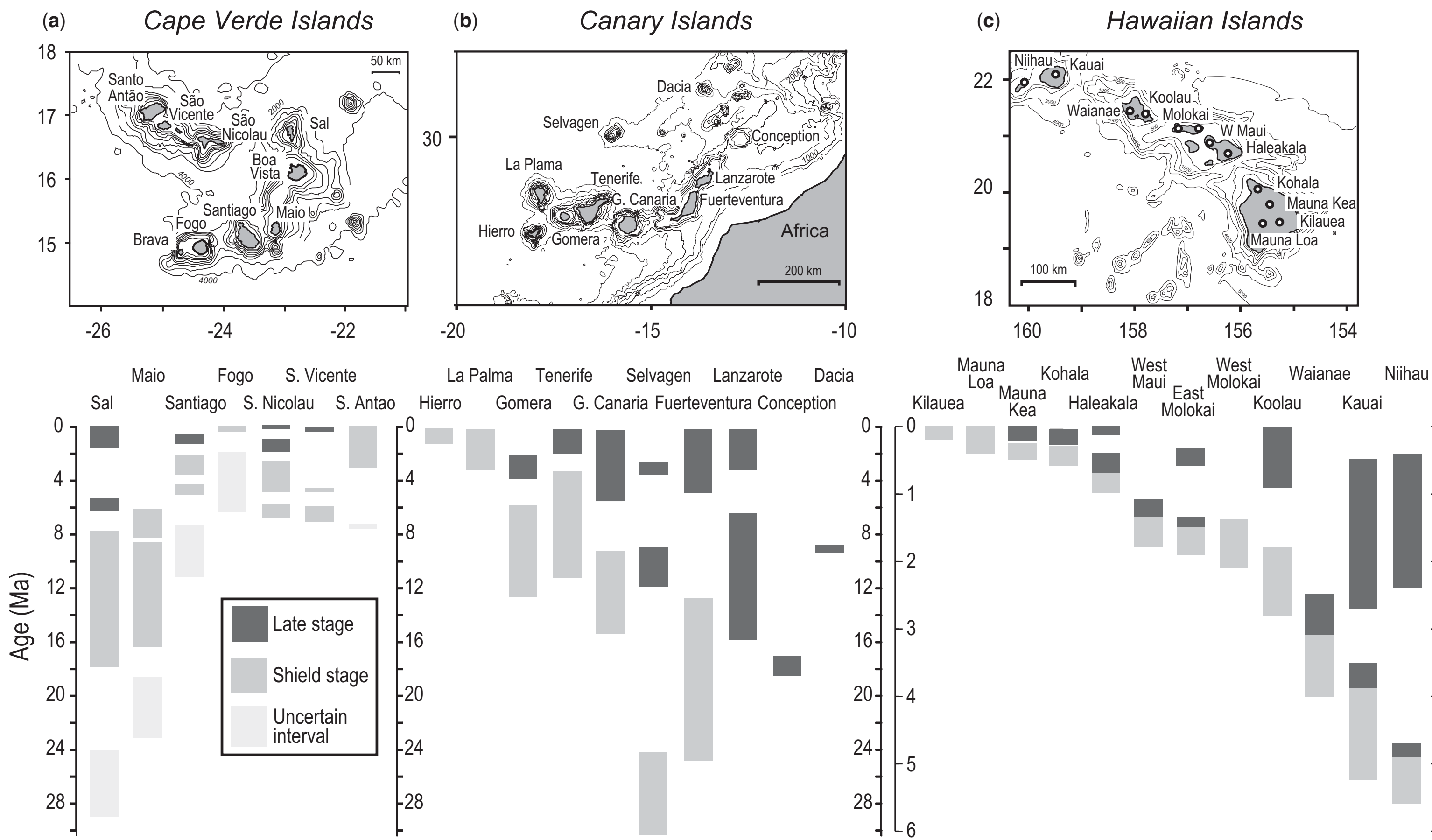

Fig. 7. Archipelago maps and age distribution (Ma) of magmatic rocks across the (**a**) Cape Verde, (**b**) Canary and (**c**) Hawaiian islands. Age distribution for the Cape Verde, Canary and Hawaiian islands modified and simplified from Holm *et al.* (2008), Geldmacher *et al.* (2001) and Clague & Dalrymple (1988), respectively. Archipelago maps for the Cape Verde, Canary Islands and Hawaiian islands are modified from Barker *et al.* (2012), Geldmacher *et al.* (2001) and Carracedo (1999), respectively.

in a higher-viscosity depleted swell root (Morgan *et al.* 1995; Yamamoto *et al.* 2007) may aid in maintaining a low subsidence rate. The emergent phase of these islands will end because of catastrophic mass-wasting processes and subsequent erosion (Carracedo 1999). Indeed, their long-term activity may result in the formation of high-relief volcanoes with steep slopes, which may evolve with time towards unstable configurations (Carracedo 1999). When unloading the lithosphere, such mass-wasting events will also strongly alter the lava chemistry and the plumbing system geometry (Manconi *et al.* 2009).

Intraplate volcanoes, such as those of the Kerguelen, Madeira and Canary islands (e.g. La Palma, El Hierro and Fogo), which are located on slow-moving plates, have a similar underground magma plumbing system geometry, with major fractionation of magmas occurring within the uppermost mantle (Fig. 8) (Amelung & Day 2002; Damaceno *et al.* 2002; Schwarz *et al.* 2004; Klugel *et al.* 2005; Scoates *et al.* 2006; Longpré *et al.* 2008; Stroncik *et al.* 2009). Magma storage and fractionation in the crust play only a minor role. Their low magma supply rates govern the geometry and the short-term longevity of the plumbing systems by controlling the thermomechanical properties of the lithosphere (Stroncik *et al.* 2009). All of these intraplate volcanoes are characterized by multistage magma ascent, with most of the fractionation processes occurring in the uppermost mantle and only short-term stagnation at shallower levels. Hence, at the Madeira and Canary islands, the plumbing systems are manifest as a plexus of small, ephemeral, partly interconnected magma chambers, sills and dykes extending from uppermost to crustal-level depths (at 430–1100 MPa: Klugel *et al.* 2005; Klugel & Klein 2006; Stroncik *et al.* 2009) (Fig. 8a).

The Cape Verde and Canary archipelagos have primary magmas, which are characterized by a wide spectrum of alkali magmatism, with a predominance of basanite–tephrite and alkali basaltic magmas, and insignificant amounts (if any) of tholeiitic melts (Kogarko & Asavin 2007). On Madeira Island, limited tholeiitic magmatism also occurs, and primary melts are mainly alkali basalts (Kogarko & Asavin 2007). The same seems to be

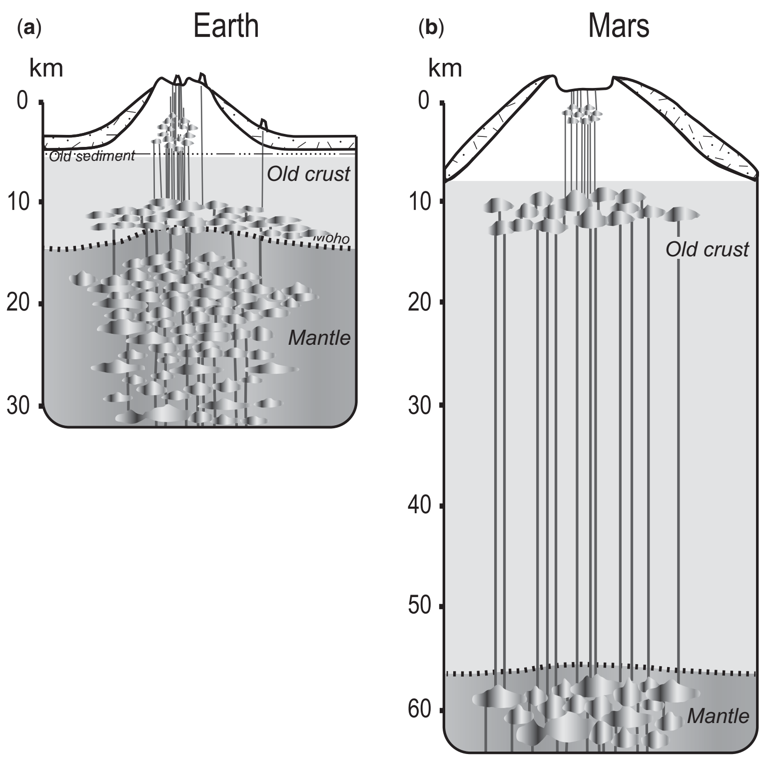

Fig. 8. Plumbing system model beneath (**a**) a terrestrial volcano from a slow-moving plate and (**b**) a Martian volcano. The magma storage systems are represented as plexuses of interconnected magma pockets and sills/dykes in the uppermost mantle and crust.

true for the Crozet (e.g. Gunn *et al.* 1970) and Kerguelen islands (e.g. Scoates *et al.* 2006). Most slow-moving plate hotspots seem to predominantly produce alkali lavas, which may be related to the presence of a thicker lithosphere in these environments. The lithosphere might be thicker as a result of its age and/or the heat loss experienced by the upwelling diapir due to intrinsically low buoyancy. Alkalic basalts may, thus, be produced by lower degrees of melting at higher pressures relative to tholeiitic basalts (Chen & Frey 1983), as the final depth of melting under a thick lithosphere will be deeper. The differentiation of tholeiitic magmas at high pressure may also be another mechanism for producing alkalic basalts under specific conditions (Albarède *et al.* 1997). Alternatively, partial melting of silica-deficient garnet pyroxenite could also be responsible for producing strongly nepheline-normative compositions (Hirschmann *et al.* 2003).

Discussion

On Earth, most of the tectonic plates are continuously regenerated and recycled through convection. The Antarctic and Nubian plates could be considered as slow surfaces of various thicknesses that are essentially not participating in the convection process but, instead, act as conductive lids on top of the much deeper convective system. This situation resembles that observed on Mars, which is characterized by a stagnant-lid regime that has been present for at least the past 4 gyr (Moresi & Solomatov 1998; Lenardic *et al.* 2004). The presence of an immobile layer, which can be modelled as a response to large viscosity contrasts in a temperature-dependent viscosity mantle, makes heat transfer out of the planetary interior dramatically less efficient than in a mobile plate tectonic regime (Reese *et al.* 1998; Hauck & Phillips 2002). Its hampering effect on mantle overturn would mainly depend on the buoyancy ratio of the system (i.e. a proxy of the relative importance of chemical to thermal buoyancy), whose consistency over the planetary evolution of Mars is doubtful. During the primordial evolution of Mars, high buoyancy values (>0.8) would have led to a thickening of the stagnant lid in response to decreasing conductive heat transfer, drastically reducing mixing efficiency compared to an isoviscous case (Tosi *et al.* 2013). However, such a stage would not last owing to the increase in compositional instability at the bottom-heated boundary layer causing a new rise in temperature, and hence activating convection until the mantle overturn stage (Elkins-Tanton *et al.* 2003; Tosi *et al.* 2013). Recent Martian mantle evolution is expected to be characterized by a lower buoyancy ratio (<0.5). When considering such buoyancy values and Rayleigh number expected for Mars (7.26×10^6: Folkner *et al.* 1997; McGovern *et al.* 2002), mixing times are longer for a stagnant-lid regime in respect to an isoviscous case (Tosi *et al.* 2013). A recent investigation of mixing times in thermochemical models of mantle convection, using the finite-element thermal convection code Ellipsis, confirmed that the recycled mixing time of a compositional anomaly, also with a strong contrast in viscosity (>50) compared with the ambient mantle, is over an order of magnitude less efficient in a stagnant-lid mode rather than in a mobile-lid mode (Debaille *et al.* 2013). On Earth, the near-immobility of the Nubian and Antarctic plates might, thus, account for the less chemically homogenized nature of South Atlantic and Indian upper-mantle reservoirs. In turn, the isotopic variability of ocean island basalts in these two provinces is much higher than that of their Pacific counterpart (Meyzen *et al.* 2007). In addition, without significant plate motion, mantle flow is primarily laminar (Bercovici *et al.* 2000). Such flow in stabilizing convective cells reduces their lateral mixing (Schmalzl *et al.* 1996). On Mars, several chemical provinces have been identified by GRS measurements at the surface (Boynton *et al.* 2007; Taylor *et al.* 2010; Baratoux *et al.* 2011), suggesting poor lateral mixing between convection cells. Such a distribution could be a direct consequence of the stagnant-lid regime. The existence of two isotopically distinct mantle provinces (South Atlantic and Indian) over the Antarctic and Nubian plates begs the question of whether this distribution also arises from a more laminar than toroidal mantle flow pattern in this area.

Owing to the stagnant-lid regime on Mars, residual depleted mantle that is left behind by the melting processes cannot be swept away from the melting locus underlying the giant Martian volcanoes. As suggested by 2D thermodynamical modelling, the residual mantle buoyancy should oppose its advection away from the top of the plume (Manglik & Christensen 1997). This situation is similar to what has been deduced from gravity and bathymetric studies for slow-moving plate hotspots by several investigators (Morgan 1995; Lodge & Helffrich 2006). The bulge observed at Tharsis could be generated due to the persistence of a stationary thick depleted layer, as suggested by Finnerty *et al.* (1988). The coupled association of both a residual layer and a thick lithosphere acts as a resistant barrier to melting processes. The final depth of melting over time is forced to higher depths and, hence, the melt production rate is reduced. Another concomitant effect of this depleted keel could be a lateral flow deflection, which would shift future melting sites (Manglik & Christensen 1997). Such a mechanism could account for the widespread distribution of volcanic centres within the Tharsis region. Finally, the formation of a depleted root at the bottom of the lithosphere might inhibit thermal erosion of the plate over time (Manglik & Christensen 1997).

Alternatively, the generation of the Tharsis bulge may be related to edge-driven convection processes. Both the Canary and Cape Verde islands lie on the same continuous basement ridge paralleling the African craton line (Patriat & Labails 2006), the formation of which has been ascribed to edge-driven convection processes (King & Ristema 2000). Such a form of convection develops as a response to large lateral gradients in lithospheric thickness and thermal structure (King & Redmond 2005). Interestingly, the Tharsis province exhibits a NE–SW-trending rise (from 50°S to 20°N) supporting the Tharsis Montes (Arsia, Pavonis and Ascraeus Montes), which is roughly parallel to the dichotomy boundary (Zuber *et al.* 2000). Its association with a broad, high aeroid anomaly (Zuber *et al.* 2000) probably mirrors the locus of upwelling of material hotter than average mantle (King & Redmond 2005). In addition, the sharpness of the dichotomy boundary suggests a short length-scale variation in crustal thickness, as observed at the West African cratonic boundary. Hence, if the early formation of the southern hemisphere domain on Mars led to the underlying development of a cratonic keel-like structure, the difference in lithospheric thickness between the northern and southern hemispheres may have led to the nucleation of small-scale, edge-driven convective instabilities, resulting in the formation of the Tharsis bulge (King & Redmond 2005).

When compared with the mean heights of Earth's hotspots as a function of lithospheric age, the Tharsis Montes (Ascraeus, Pavonis and Arsia) lie in the extension of the trend defined by motionless plate hotspots (less than 25 mm a^{-1}: Figs 2 & 9). To first order, one could infer that in the absence of plate movement, the melting region remains geographically fixed with time, and melts accumulate to form large swell heights (Figs 2 & 9). However, the crustal thickness is variable beneath the Tharsis Montes. It is more likely that these large swells, as well as those observed for motionless plate hotspots, are supported both by the presence of a thick, stationary, residual-depleted layer/keel, produced by melting processes, and by large-scale mantle upwellings. Therefore, understanding the mechanisms that generate oceanic swells at motionless plates is pivotal to future progress in our knowledge of plume-fed building processes at Tharsis.

Owing to the low gravity on Mars, fluid convection flows (and consequent convective heat transfer) and crystal settling processes will be slower than on

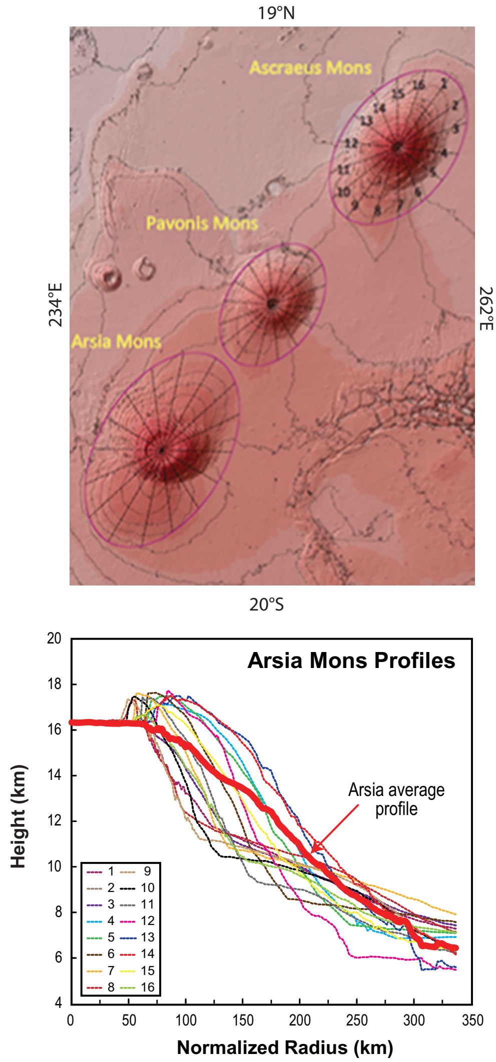

Fig. 9. (**a**) Profile locations across Pavonis, Ascraeus and Arsia Montes. (**b**) Topographical profiles for Arsia Mons. Sixteen profiles with the axis of symmetry centred on the main caldera were extracted for each volcano. In order to eliminate the ellipticity of the edifices, the profiles were normalized to the average radius. An average height profile was, thus, extracted using Origin Pro software. This procedure was used to obtain the most representative topographical profile for each volcano.

Earth (Wilson & Head 1994). Consequently, upwellings will have an intrinsically low buoyancy flux, and their ascent rates will be slow. Such features are shared by some slow-moving plate plumes, such as the Crozet hotspot, because of their low buoyancy fluxes. Uranium disequilibrium studies indicate that these weaker hotspots will also be characterized by lower excess temperatures than stronger hotspots such as Hawaii (Bourdon *et al.* 2006), as they cool more during upwelling (Albers & Christensen 1996). Their upwelling ascension rates will even be more reduced if water is present. Melting induces a dehydration of the mantle upwelling, which increases its viscosity by a factor of 7 and drastically reduces its velocity (Bourdon *et al.* 2006). Such inferences may also partially hold for the Tharsis volcanoes, for which the estimated mantle potential temperatures (i.e. the temperature that mantle peridotite would have if it ascended adiabatically to the surface without melting; 1335–1380 °C: Baratoux *et al.* 2011) fall in the range of those calculated for average ambient mantle and weak plumes (Herzberg & Gazel 2009). This factor could then be superimposed on Martian mantle cooling over time (Baratoux *et al.* 2011).

A major difference between terrestrial and Martian edifices concerns the greater depth interval between the depths of melting and crystallization for volcanoes on Mars relative to those on Earth. On Mars, melting terminates at much greater depths owing to the presence of a thick lithosphere (110–160 km: Baratoux *et al.* 2011). Two processes may contribute to the thickening of the Martian lithosphere: (1) the lithosphere may thicken over time due to the formation of a residual depleted layer in the absence of plate movement; and (2) the low buoyancy of upwelling leads to enhanced heat loss and, thus, to a termination of melting at deeper levels and the formation of a thick lithosphere. Such a situation would be similar to that of terrestrial plumes rising below an old and thick oceanic lithosphere (e.g. at the Canary or Crozet archipelago). As a consequence, quantifying the lithospheric thickness and its influence on melting processes in these environments will help to understand the shape of the mantle melting regime on Mars.

Again, owing to the lower gravity on Mars, magma chambers are expected to be much larger and deeper than their counterparts on Earth in order to avoid cooling and solidification, and to supply magma to the surface (Wilson & Head 1994). Intrusives are expected to be common, but have yet to be discovered. The lower buoyancy forces and the deeper levels of neutral buoyancy would seem to favour the development of magma diapirs and dykes at depth. Loss of heat by diffusion of the rising diapir will also favour the retention and crystallization of melt in the uppermost mantle. Such a mechanism has been inferred for Ascraeus Mons by Pozzobon *et al.* (2014) through fractal analysis of alignments of pit craters. Interestingly, the plumbing system of Ascraeus appears to be similar to that observed for motionless plate volcanoes, where most of the fractionation occurs in the uppermost mantle. A second level of fractionation proceeds in the lower crust and minor crystallization develops at shallow depths within the volcano, just underneath the summit (Fig. 8).

Another common characteristic between volcanoes on slow-moving plates and those on Tharsis is their great volcanic longevity, inherited from their stationary position relative to the assumed melting source. Hence, some Canary (e.g. Gomera: Geldmacher *et al.* 2001) and Cape Verde volcanoes (e.g. Sal: Holm *et al.* 2008) are active for more than 10 myr (Fig. 7), while the longest period of prolonged though episodic activity for volcanoes of Tharsis is up to 1 gyr (Robbins *et al.* 2011; Grott *et al.* 2013) (Fig. 3). The volcanic lifetimes of Martian shields are much longer than those of the prototypical Hawaiian Islands (Fig. 7). The early history of Mars was marked by intense volcanism at least during the late Noachian, with the activity gradually weakening over time. This overall decline was punctuated by episodic periods of high volcanic intensity (Wilson *et al.* 2001; Neukum *et al.* 2004). In particular, Tharsis volcanoes might have been built episodically with active phases lasting less than 1 myr alternating with 100 myr quiet phases (Wilson *et al.* 2001). The occurrence of long periods of quiescence, which separate magmatic stages, also seems to be a defining characteristic of the evolutionary histories of volcanoes from motionless plates. Indeed, most volcanoes at Cape Verde (e.g. Holm *et al.* 2008) and the Canary Islands (e.g. Geldmacher *et al.* 2001) have histories of sporadic activity with chronological gaps of up to 12 myr (e.g. Selvagen Island: Geldmacher *et al.* 2001), much longer than those observed at Hawaii (Fig. 7). Understanding the evolution of volcanoes at motionless plates on Earth will, thus, help to decipher the mechanisms governing the effusion history at Tharsis.

Effusion rates primarily reflect spatial and temporal variations in melting extents, which can be induced by changes in mantle potential temperature, thickness of the overlying lithosphere and/or mantle composition. The effusive rate of approximately 0.04 $km^3\,a^{-1}$ (Greeley & Schneid 1991) determined for early activity (Noachian–Hesperian) in Martian volcanic provinces is higher than that calculated during the Amazonian (*c.* 0.01 $km^3\,a^{-1}$: Fig. 6). When the eruption rate for this latter period is compared to those of present-day plumes on Earth, it is found to be drastically lower than that of Hawaiian Islands and closer to some of the values observed for slow-moving plate hotspots (e.g. Canary, Madeira: Fig. 6).

Some volcanoes at near-stationary plates tend to be rugged with steep slopes, such as those observed on the Crozet and Canary islands. Owing to their steeper slopes, these high-relief volcanoes may develop with time towards unstable configurations (e.g. Carracedo 1999). Catastrophic flank failures and collapses may thus occur more frequently than in the Hawaiian Islands, with their concomitant effects on lava chemistry and plumbing system geometry (Manconi *et al.* 2009). Conversely, large Martian volcanoes were primarily affected by pronounced sagging due to load-induced lithospheric flexure (McGovern & Solomon 1993; Byrne *et al.* 2009, 2013). This led to a general compressional environment on the flanks of the volcanoes, preventing mass-wasting events and generating typical imbricate lobate terraces bounded by thrust faults (Thomas *et al.* 1990; Byrne *et al.* 2009). Actually, prominent gravitational collapses have been documented only at the foot of Olympus Mons, which might have spread over a basal décollement causing oversteepening of lower slopes; meanwhile, upper flanks continued to be shortened due to edifice sagging (Byrne *et al.* 2013). However, such characteristic net compression on Martian volcanoes is not likely in the later stages of their development (Amazonian age) as a result of the lithosphere thickening over time. This is well proven for Ascraeus Mons, where compression transitioned to extension (not necessarily related to gravitational collapse) through time (Byrne *et al.* 2012).

Average surface heat fluxes for Tharsis volcanoes (22–26 mW m^{-2}: Grott *et al.* 2013) are much lower than those observed on Earth for slow-moving plate hotspots (63–96 mW m^{-2}: Harris & McNutt 2007). However, if hot mantle wells up under the Tharsis province, the size and strength of such a plume, as predicted from the modelling of the elastic thickness and maximum average heat flux of Tharsis Montes (8–24 mW m^{-2}), would yield central peak heat flux values ranging from 40 up to 120 mW m^{-2} (Grott & Breuer 2010). These calculated values clearly encompass the range of those measured at terrestrial hotspots located on motionless plates. The Discovery-class mission *InSight* (Banerdt *et al.* 2012), scheduled to launch in 2016 to perform *in situ* measurements of heat flow at the Martian surface, may allow the validity of this assumption to be tested (Spohn *et al.* 2012).

Although *in situ* measurements do not exist for the Tharsis province, widespread GRS and thermal emission spectrometer (TES) data and soil analyses (e.g. Gusev Crater, Meridiani Planum: McSween *et al.* 2009) suggest that volcanism on Mars is predominantly of tholeiitic nature, and results from extensive partial melting. Such a composition constitutes a primary difference to intraplate volcanism at slow-moving plates, which mostly consists of erupted Ne-normative alkali basalts (Kogarko & Asavin 2007). However, recent analyses performed by the Mars Science Laboratory at Gale Crater may challenge this view, as a mugearite-like rock was identified (Stolper *et al.* 2013). This rock may have fractionated either from a primary alkaline or a transitional magma, which has been produced by the melting of a mantle source distinct from those of other known Martian basalts (Stolper *et al.* 2013). Future exploration may document other

Table 1. *Similarities and differences between volcanoes from slow- and fast-motion plates and the volcanic provinces on Mars*

Features	Slow-motion plate hotspots	Mars volcanic provinces (Tharsis)	Fast-motion plate hotspots (Hawaii)
Great height of volcanic bulge/swell	Yes	Yes	No
Sagging processes due to self-loading and lithospheric flexure	No?	Yes (only at the early stage)	Yes
Age-progressive chains of volcanoes	No (<30 Ma)	No	Yes
Long-lasting volcanic activity punctuated by large temporal gaps	Yes	Yes	No
Alkali volcanism	Yes	Possible	Yes (except for the shield stage)
Two-level architecture of the plumbing system during the shield stage with most fractionation in the uppermost mantle	Yes	Yes	No
Lithosphere thickening due to:			
– The formation of a stationary residual mantle lid	Yes	Yes	No
– Low buoyancy of upwelling			
Slow convection mixing	Yes	Yes	No
High heat fluxes	Yes	Yes	No

alkaline suites on Mars, which could further reinforce the appropriateness of viewing volcanoes on motionless plates as analogues to Martian volcanoes.

Conclusion

On Earth, many geodynamic features of young volcanism (less than 30 myr old) in motionless intraplate oceanic island environments resemble those of Mars, where plate tectonics plays no meaningful role in shaping planetary geodynamics. Mars can effectively be considered as a one-plate planet, where geodynamics processes occur within a stagnant-lid regime. Several features of volcanism both on Earth and on Mars can be related to the (near-) absence of plate tectonic motion (Table 1).

The dividing of the mantle into several distinct chemical provinces, as proposed for Mars and over the Antarctic and Nubian plates on Earth, reflects a more efficient intracell rather than cross-cell convection mixing, allowing preservation of large-scale mantle chemical heterogeneities. Such a pattern reflects a mantle flow regime dominated by laminar flow, as expected in the (near-) absence of plate tectonic motion.

In these geodynamic environments, poor residual mantle lateral-flowing traction from the melting site will lead to the formation of a near-stationary depleted layer, which will thicken with time. The low buoyancy of upwelling in enhancing conductive heat loss during mantle rising will also lead to the formation of a thicker lithosphere relative to that of overlying higher-buoyancy plumes, such as Hawaii. These two thickening effects add to that due to planetary cooling (Baratoux *et al.* 2011). Both planetary cooling and depleted lid formation will lead to a cessation of melting, progressively forced towards greater depths over time, while the average extent of melting will be reduced. In both environments, low melt supply will lead to the development of a two-level fractionation architecture of the plumbing system, with most of the fractionation occurring in the uppermost mantle.

The widespread distribution of the Tharsis volcanoes, as well as the horseshoe-like shape of some volcanic islands on slow-moving plates (e.g. Cape Verde, Crozet), could be inherited from lateral-flow deflection induced by the presence of a residual mantle keel, shifting future melting loci around the keel. The pronounced topographical swells/bulges observed in this environment may also be supported both by large-scale mantle upwelling and by their residual mantle roots.

Another similarity between volcanoes on slow-moving plates and those in Tharsis is their great longevity, which is due to their stationary position relative to the melting source. Both sets of volcanoes also have a history of protracted activity punctuated by long periods of quiescence. The accumulation of refractory material at the rim of their melting zones might play a role in the fluctuations of their long-term volcanic activity.

Until now, volcanism on Mars was defined as being predominantly of tholeiitic composition. However, recent *in situ* analyses at Gale Crater have identified a mugearite-like rock. This raises the possibility that both intraplate volcanism on Earth at slow-moving plates and that on Mars would, instead, be of an alkali nature.

Our knowledge of terrestrial volcanoes from motionless plates can thus help us to better understand the nature and significance of large-scale melting and differentiation processes of volcanoes on Mars. However, the extent of this knowledge is still insufficiently detailed in many respects, and requires further investigation. New data from the Martian planetary record will help to provide new perspectives on the processes and evolution of volcanoes on near-stationary plates. On Mars, the large range of scales of upwelling, and the influence of crustal and lithospheric thicknesses in space and time, are thus relevant to studies of hotspots on motionless plates.

Two anonymous reviewers are gratefully acknowledged for their thorough and constructive reviews that helped to improve the manuscript. We also thank Thomas Platz and Paul K. Byrne for their editorial comments. This project was supported by an ATENEO grant CPDA114007/11.

References

Albarède, F., Luais, B. *et al.* 1997. The geochemical regime of Piton de la Fournaise volcano (Réunion) during the last 530 000 years. *Journal of Petrology*, **38**, 171–201.

Albers, M. & Christensen, U. R. 1996. The excess temperature of plumes rising from the core-mantle boundary. *Geophysical Research Letters*, **23**, 3567–3570.

Ali, M. Y., Watts, A. B. & Hill, I. 2003. A seismic reflection profile study of lithospheric flexure in the vicinity of the Cape Verde islands. *Journal of Geophysical Research*, **108**, 2239, http://dx.doi.org/10.1029/2002JB002155

Amelung, F. & Day, S. 2002. Insar observations of the 1995 Fogo, Cape Verde, eruption: implications for the effects of collapse events upon island volcanoes. *Geophysical Research Letters*, **29**, 1606, http://dx.doi.org/10.1029/2001GL013760

Argus, D. F., Gordon, R. G. & DeMets, C. 2011. Geologically current motion of 56 plates relative to the no-net-rotation reference frame. *Geochemistry, Geophysics, Geosystems*, **12**, Q11001, http://dx.doi.org/10.1029/2011GC003751

Banda, E., Dafiobeitia, J. J., Surifiach, E. & Ansorge, J. 1981. Features of crustal structure under the Canary islands. *Earth and Planetary Science Letters*, **55**, 11–24.

Banerdt, W. B., Smrekar, S. E. *et al.* 2012. Insight: an integrated exploration of the interior of Mars. Paper 2838, presented at the 43rd Lunar and Planetary Science Conference, 19–23 March 2012, The Woodlands, TX.

Baratoux, D., Toplis, M. J., Monnereau, M. & Gasnault, O. 2011. Thermal history of Mars inferred from orbital geochemistry of volcanic provinces. *Nature*, **472**, 338–341.

Bargar, K. E. & Jackson, E. D. 1974. Calculated volumes of individual shield volcanoes along the Hawaiian–Emperor Chain. *Journal of Research of the United States Geological Survey*, **2**, 545–550.

Barker, A. K., Troll, V. R., Ellam, R. M., Hansteen, T. H., Harris, C., Stillman, C. J. & Andersson, A. 2012. Magmatic evolution of the Cadamosto seamount, Cape Verde: beyond the spatial extent of EM1. *Contributions to Mineralogy and Petrology*, **163**, 949–965.

Bercovici, D., Ricard, Y. & Richards, M. A. 2000. The relation between mantle dynamics and plate tectonics: a primer in the history and dynamics of global plate motions. *In*: Richards, M. A., Gordon, R. G. & Van der Hilst, R. D. (eds). *The History and Dynamics of Global Plate Motions*. American Geophysical Union, Geophysical Monograph, **121**, 5–46.

Bleacher, J. E., Greeley, R., Williams, D. A., Werner, S. C., Hauber, E. & Neukum, G. 2007. Olympus Mons, Mars: inferred changes in late Amazonian aged effusive activity from lava flow mapping of Mars express high resolution stereo camera data. *Journal of Geophysical Research*, **112**, E04003, http://dx.doi.org/10.1029/2006JE002826

Bourdon, B., Ribe, N. M., Stracke, A., Saal, A. E. & Turner, S. P. 2006. Insights into the dynamics of mantle plumes from uranium-series geochemistry. *Nature*, **444**, 713–7.

Bouvier, A., Blichert-Toft, J. & Albarède, F. 2009. Martian meteorite chronology and the evolution of the interior of Mars. *Earth and Planetary Science Letters*, **280**, 285–295.

Boynton, W. V., Taylor, G. J. *et al.* 2007. Concentration of H, Si, Cl, K, Fe, and Th in the low- and mid-latitude regions of Mars. *Journal of Geophysical Research*, **112**, E12, http://dx.doi.org/10.1029/2007JE002887

Buske, M. 2006. *Three-dimensional thermal evolution models for the interior of Mars and Mercury*. PhD thesis, Georg-August-University, Göttingen.

Byrne, P. K., van Wyk de Vries, B., Murray, J. B. & Troll, V. R. 2009. The geometry of volcano flank terraces on Mars. *Earth and Planetary Science Letters*, **281**, 1–13.

Byrne, P. K., van Wyk de Vries, B., Murray, J. B. & Troll, V. R. 2012. A volcanotectonic survey of Ascraeus Mons, Mars. *Journal of Geophysical Research*, **117**, E01004, http://dx.doi.org/10.1029/2011JE003825

Byrne, P. K., Holohan, E. P., Kervyn, M., van Wyk de Vries, B., Troll, V. R. & Murray, J. B. 2013. A sagging-spreading continuum of large volcano structure. *Geology*, **41**, 339–342, http://dx.doi.org/10.1130/G33990.1

Canales, J. P. & Danobeitia, J. J. 1998. The Canary Islands swell: a coherence analysis of bathymetry and gravity. *Geophysical Journal International*, **132**, 479–488.

Carr, M. H. 2006. *The Surface of Mars*. Cambridge University Press, Cambridge.

Carr, M. H. & Head, J. W., III . 2010. Geologic history of Mars. *Earth and Planetary Science Letters*, **294**, 185–203.

Carracedo, J. C. 1999. Growth, structure, instability and collapse of Canarian volcanoes and comparisons with Hawaiian volcanoes. *Journal of Volcanology and Geothermal Research*, **94**, 1–19.

Cazenave, A., Dominh, K., Rabinowicz, M. & Ceuleneer, G. 1988. Geoid and depth anomalies over ocean swells and troughs: evidence of an increasing trend of the geoid to depth ratio with age of plate. *Journal of Geophysical Research*, **93**, 8064–8077.

Charvis, P., Recq, M., Operto, S. & Brefort, D. 1995. Deep structure of the northern Kerguelen plateau and hotspot-related activity. *Geophysical Journal International*, **122**, 899–924.

Chen, C.-Y. & Frey, F. A. 1983. Origin of Hawaiian tholeiite and alkali basalt. *Nature*, **302**, 785–789.

Clague, D. A. & Dalrymple, G. B. 1988. Age and petrology of alkalic postshield and rejuvenated-stage lava from Kauai, Hawaii. *Contributions to Mineralogy and Petrology*, **99**, 202–218.

Courtney, R. & Recq, M. 1986. Anomalous heat flow near the Crozet plateau and mantle convection. *Earth and Planetary Science Letters*, **79**, 373–384.

Courtney, R. C. & White, R. S. 1986. Anomalous heat flow and geoid across the Cape Verde rise: evidence for dynamic support from a thermal plume in the mantle. *Geophysical Journal of the Royal Astronomical Society*, **87**, 815–867.

Crumpler, L. S., Head, J. W. & Aubele, J. C. 1996. Calderas on Mars: characteristics, structure, and associated flank deformation. *In*: McGuire, W. J., Jones, A. P. & Neuberg, J. (eds) *Volcano Instability on the Earth and Other Planets*. Geological Society, London, Special Publications, **110**, 307–348.

Damasceno, D., Scoates, J. S., Weiss, D., Frey, F. A. & Giret, A. 2002. Mineral chemistry of midly alkalic basalts from the 25 ma Mont Crozier section, Kerguelen archipelago: constraints on phenocryst crystallization environments. *Journal of Petrology*, **43**, 1389–1413.

Debaille, V., O'Neill, C., Brandon, A. D., Haenecour, P., Yin, Q.-Z., Mattielli, N. & Treiman, A. H. 2013. Stagnant-lid tectonics in early Earth revealed by ^{142}Nd variations in late Archean rocks. *Earth and Planetary Science Letters*, **373**, 83–92.

Detrick, R. S. & Crough, S. T. 1978. Island subsidence, hot spots, and lithospheric thinning. *Journal of Geophysical Research*, **83**, 1236–1244.

Elkins-Tanton, L., Parmentier, E. & Hess, P. 2003. Magma ocean fractional crystallization and cumulate overturn in terrestrial planets: implications for Mars. *Meteoritics and Planetary Science*, **38**, 1753–1771.

El Maarry, M. R., Gasnault, O. *et al.* 2009. Gamma-ray constraints on the chemical composition of the Martian surface in the Tharsis region: a signature of partial melting of the mantle? *In*: Bleacher, J. E. & Dohm, J. M. (eds) *Tectonic and Volcanic History of the Tharsis Province, Mars*. *Journal of Volcanology and Geothermal Research*, **185**, 116–122.

Filmer, P. E. & McNutt, M. K. 1989. Geoid anomalies over the Canary Islands group. *Marine Geophysical Researches*, **11**, 77–87.

Finnerty, A. A., Phillips, R. J. & Banerdt, W. B. 1988. Igneous processes and closed system evolution of the Tharsis region of Mars. *Journal of Geophysical Research*, **93**, 10,225–10,235.

Folkner, W. M., Yoder, C. F., Yuan, D. N., Standish, E. M. & Preston, R. A. 1997. Interior structure and seasonal mass redistribution of Mars from radio tracking of Mars Pathfinder. *Science*, **278**, 1749–1752.

Funck, T. & Schmincke, H.-U. 1998. Growth and destruction of Gran Canaria deduced from seismic reflection and bathymetric data. *Journal of Geophysical Research*, **103**, 15,393–15,407.

Gasnault, O., Taylor, G. J. *et al.* 2010. Quantitative geochemical mapping of Martian elemental provinces. *Icarus*, **207**, 226–247.

Geldmacher, J., Van den Bogaard, P., Hoernle, K. & Schmincke, H.-U. 2000. The ^{40}Ar/^{39}Ar age dating of the Madeira archipelago and hotspot track (Eastern North Atlantic). *Geochemistry, Geophysics, Geosystems*, **1**, 1008, http://dx.doi.org/10.1029/1999GC000018

Geldmacher, J., Hoernle, K., Van den Bogaard, P., Zankl, G. & Garbe-Schönberg, D. 2001. Earlier history of the $\leq$70-ma-old Canary hotspot based on the temporal and geochemical evolution of the Selvagen archipelago and neighboring seamounts in the Eastern North Atlantic. *Journal of Volcanology and Geothermal Research*, **111**, 55–87.

Giacomini, L., Massironi, M., Martellato, E., Pasquare, G., Frigeri, A. & Cremonese, G. 2009. Inflated flowson Daedalia Planum (Mars)? Clues from a comparative analysis with the Payen volcanic complex (Argentina). *Planetary and Space Science*, **57**, 556–570.

Golabek, G. J., Keller, T., Gerya, T. V., Zhu, G., Tackley, P. J. & Connolly, J. A. D. 2011. Origin of the Martian dichotomy and Tharsis from a giant impact causing massive magmatism. *Icarus*, **215**, 346–357.

Golle, O., Dumoulin, C., Choblet, G. & Cadek, O. 2012. Topography and geoid induced by a convecting mantle beneath an elastic lithosphere. *Geophysical Journal International*, **189**, 55–72.

Greeley, R. & Schneid, B. D. 1991. Magma generation on Mars – amounts, rates, and comparisons with Earth, Moon, and Venus. *Science*, **254**, 996–998.

Grevemeyer, I. 1999. Isostatic geoid anomalies over mid-plate swells in the central north Atlantic. *Geodynamics*, **28**, 41–50.

Grott, M. & Breuer, D. 2009. Implications of large elastic thicknesses for the composition and current thermal state of Mars. *Icarus*, **201**, 540–548.

Grott, M. & Breuer, D. 2010. On the spatial variability of the Martian elastic lithosphere thickness: evidence for mantle plumes? *Journal of Geophysical Research*, **115**, 1–16.

Grott, M., Baratoux, D. *et al.* 2013. Long-term evolution of the Martian crust-mantle system. *Space Science Reviews*, **174**, 49–111.

Gunn, B. M., Coy-Yll, R., Watkins, N. D., Abranson, C. E. & Nougier, J. 1970. Geochemistry of an oceanite-ankaramite-basalt suite from East Island, Crozet archipelago. *Contributions to Mineralogy and Petrology*, **28**, 319–339.

Harder, H. 2000. Mantle convection and the dynamic geoid of Mars. *Geophysical Research Letters*, **27**, 301–304.

Harris, R. N. & McNutt, M. K. 2007. Heat flow on hot spot swells: evidence for fluid flow. *Journal of Geophysical Research*, **112**, B3, http://dx.doi.org/10.1029/2006JB004299

Hartmann, W. K. & Neukum, G. 2001. Cratering chronology and the evolution of Mars. *Space Science Reviews*, **96**, 165–194.

Hauber, E., Brož, P., Jagert, F., Jodlowski, P. & Platz, T. 2011. Very recent and wide-spread basaltic volcanism on Mars. *Geophysical Research Letters*, **38**, 10, http://dx.doi.org/10.1029/2011GL047310

Hauck, S. A., II & Phillips, R. J. 2002. Thermal and crustal evolution of Mars. *Journal of Geophysical Research*, **107**, 5052, http://dx.doi.org/10.1029/2001JE001801

Herzberg, C. & Gazel, E. 2009. Petrological evidence for secular cooling in mantle plumes. *Nature*, **458**, 619–622.

Hiesinger, H., Head, J. W., III & Neukum, G. 2007. Young lava flows on the eastern flank of Ascraeus Mons: rheological properties derived from high resolution stereo camera (HRSC) images and Mars orbiter laser altimeter (MOLA) data. *Journal of Geophysical Research*, **112**, E5, http://dx.doi.org/10.1029/2006JE002717

Hirschmann, M. M., Kogiso, T., Baker, M. B. & Stolper, E. M. 2003. Alkalic magmas generated by partial melting of garnet pyroxenite. *Geology*, **31**, 481–484.

Hoernle, K. & Schmincke, H.-U. 1993. The petrology of the tholeiites through melilite nephelinites on Gran Canaria, Canary Islands: crystal fractionation, accumulation, and depth of melting. *Journal of Petrology*, **34**, 573–578.

Holm, P. M., Grandvuinet, T., Friis, J., Wilson, J. R., Barker, A. K. & Plesner, S. 2008. An ^{40}Ar–^{39}Ar study of the Cape Verde hot spot: temporal evolution in a semistationary plate environment. *Journal of Geophysical Research*, **113**, B08201, http://dx.doi.org/10.1029/2007JB005339

Jung, W.-Y. & Rabinowitz, P. D. 1986. Residual geoid anomalies of the North Atlantic Ocean and their tectonic implications. *Journal of Geophysical Research*, **91**, 10,383–10,396.

Keller, T. & Tackley, P. J. 2009. Towards self-consistent modeling of the Martian dichotomy: the influence of one-ridge convection on crustal thickness distribution. *Icarus*, **202**, 429–443.

King, S. D. & Redmond, H. L. 2005. The crustal dichotomy and edge driven convection: a mechanism for Tharsis rise volcanism? Abstract 1960, presented at the 36th Annual Lunar and Planetary Science Conference, 14–18 March 2005, League City, TX.

King, S. D. & Ritsema, J. 2000. African hot spot volcanism: small-scale convection in the upper mantle beneath cratons. *Science*, **290**, 1137–1140.

Klugel, A. & Klein, F. 2006. Complex magma storage and ascent at embryonic submarine volcanoes from Madeira archipelago. *Geology*, **34**, 337–340.

Klugel, A., Hansteen, T. H. & Galipp, K. 2005. Magma storage and underplating beneath Cumbre Vieja volcano, la Palma (Canary islands). *Earth and Planetary Science Letters*, **236**, 211–226.

Kogarko, L. N. & Asavin, A. M. 2007. Regional features of primary alkaline magmas of the Atlantic Ocean. *Geochemistry International*, **45**, 841–856.

Lenardic, A., Nimmo, F. & Moresi, L. 2004. Growth of the hemispheric dichotomy and the cessation of plate tectonics on Mars. *Journal of Geophysical Research*, **109**, E02, http://dx.doi.org/10.1029/2003JE002172

Lin, J. 1998. Hitting the hotspots. *Oceanus*, **41**, 34–37.

Liu, M. & Chase, C. G. 1989. Evolution of midplate hotspot swells: numerical solutions. *Journal of Geophysical Research*, **94**, 5571–5584.

Lodge, A. & Helffrich, G. 2006. Depleted swell root beneath the Cape Verde islands. *Geology*, **34**, 449–452.

Longpré, M.-A., Troll, V. R. & Hansteen, T. H. 2008. Upper mantle magma storage and transport under a Canarian shield-volcano, Teno, Tenerife (Spain). *Journal of Geophysical Research*, **113**, B08203, http://dx.doi.org/10.1029/2007JB005422

Manconi, A., Longpré, M.-A., Walter, T. R., Troll, V. R. & Hansteen, T. H. 2009. The effects of flank collapses on volcano plumbing systems. *Geology*, **37**, 1099–1102.

Manglik, A. & Christensen, U. R. 1997. Effect of mantle depletion buoyancy on plume flow and melting beneath a stationary plate. *Journal of Geophysical Research*, **102**, 5019–5028.

Marks, K. M. & Sandwell, D. T. 1991. Analysis of geoid height versus topography for oceanic plateaus and swells using nonbiased linear regression. *Journal of Geophysical Research*, **96**, 8045–8055.

McGovern, P. J. & Morgan, J. K. 2009. Volcanic spreading and lateral variations in the structure of Olympus Mons, Mars. *Geology*, **37**, 139–142.

McGovern, P. J. & Solomon, S. C. 1993. State of stress, faulting, and eruption characteristics of large volcanoes on Mars. *Journal of Geophysical Research*, **98**, 23,553–23,579.

McGovern, P. J., Solomon, S. C. *et al.* 2002. Localized gravity/topography admittance and correlation spectra on Mars: implications for regional and global evolution. *Journal of Geophysical Research*, **107**, E12, http://dx.doi.org/10.1029/2002JE001854

McSween, H. Y. J., Taylor, G. J. & Wyatt, M. B. 2009. Elemental composition of the Martian crust. *Science*, **324**, 736–739.

Meyzen, C. M., Ludden, J., Humler, E., Mével, C. & Albarède, F. 2007. Isotopic portrayal of the upper mantle flow field. *Nature*, **447**, 1069–1074.

Monnereau, M. & Cazenave, A. 1990. Depth and geoid anomalies over oceanic hotspot swells: a global survey. *Journal of Geophysical Research*, **95**, 15,429–15,438.

Moore, J. G. & Campbell, J. F. 1987. Age of tilted reefs, Hawaii. *Journal of Geophysical Research*, **92**, 2641–2646.

Moresi, L. & Solomatov, V. S. 1998. Mantle convection with a brittle lithosphere: thoughts on the global tectonic style of the Earth and Venus. *Geophysical Journal International*, **133**, 669–682.

Morgan, J. P., Morgan, W. J. & Price, E. 1995. Hotspot melting generates both hotspot volcanism and a hotspot swell? *Journal of Geophysical Research*, **100**, 8045–8062.

Mouginis-Mark, P. J. & Robinson, M. S. 1992. Evolution of the Olympus Mons Caldera, Mars. *Bulletin of Volcanology*, **54**, 347–360.

Neukum, G., Jaumann, R. *et al.* 2004. Recent and episodic volcanic and glacial activity on Mars revealed by the high resolution stereo camera. *Nature*, **432**, 971–979.

Newsom, H. E., Crumpler, L. S. *et al.* 2007. Geochemistry of Martian soil and bedrock in mantled and less mantled terrains with gamma ray data from Mars odyssey. *Journal of Geophysical Research*, **112**, E3, http://dx.doi.org/10.1029/2006JE002680

Olson, P. 1990. Hot spots, swells, and mantle plumes. *In*: Ryan, M. P. (ed.) *Magma Transport and Storage*. Wiley, New York, 33–51.

Patriat, M. & Labails, C. 2006. Linking the Canary and Cape-Verde hot-spots, northwest Africa. *Marine Geophysical Researches*, **27**, 201–215.

Phillips, R. J., Sleep, N. H. & Banerdt, W. B. 1990. Permanent uplift in magmatic systems with application to the Tharsis region of Mars. *Journal of Geophysical Research*, **95**, 5089–5100.

Phillips, R. J., Zuber, M. T. *et al.* 2001. Ancient geodynamics and global-scale hydrology on Mars. *Science*, **291**, 2587–2591.

Pim, J., Peirce, C., Watts, A. B., Grevemeyer, I. & Krabbenhoeft, A. 2008. Crustal structure and origin of the Cape Verde rise. *Earth and Planetary Science Letters*, **272**, 422–428.

Pozzobon, R., Mazzarini, F., Massironi, M. & Marinangeli, L. 2014. Self-similar clustering distribution of structural features on Ascraeus Mons (Mars): implications for magma chamber depth. *In*: Platz, T., Massironi, M., Byrne, P. K. & Hiesinger, H. (eds) *Volcanism and Tectonism Across the Inner Solar System*. Geological Society, London, Special Publications, **401**. First published online March 25, 2014, http://dx.doi.org/10.1144/SP401.12

Plescia, J. B. 2004. Morphometric properties of Martian volcanoes. *Journal of Geophysical Research*, **109**, E3, http://dx.doi.org/10.1029/2002JE002031

Recq, M. & Charvis, P. 1987. La ride asismique de Kerguelen-Heard – anomalie du géoide et compensation isostatique. *Marine Geology*, **76**, 301–311.

Recq, M., Le Roy, I., Charvis, P., Goslin, J. & Brefort, D. 1990. Structure profonde du Mont Ross d'après la réfraction sismique (les Kerguelen, Océan Indien Austral). *Canadian Journal of Earth Sciences*, **31**, 1806–1821.

Recq, M., Goslin, J., Charvis, P. & Operto, S. 1998. Small-scale crustal variability within an intraplate structure: the Crozet bank (Southern Indian Ocean). *Geophysical Journal International*, **134**, 145–156.

Reese, C. C., Solomatov, V. S. & Moresi, L.-N. 1998. Heat transport efficiency for stagnant lid convection with dislocation viscosity: application to Mars and Venus. *Journal of Geophysical Research*, **103**, 13 643–13 657.

Ribe, N. M. & Christensen, U. R. 1994. 3-dimensional modeling of plume lithosphere interaction. *Journal of Geophysical Research*, **99**, 669–682.

Robbins, S. J., Di Achille, G. & Hynek, B. M. 2011. The volcanic history of Mars: high-resolution crater-based studies of the calderas of 20 volcanoes. *Icarus*, **211**, 1179–1203.

Roberts, J. H. & Zhong, S. J. 2006. Degree-1 convection in the Martian mantle and the origin of the hemispheric dichotomy. *Journal of Geophysical Research*, **111**, E06013, http://dx.doi.org/10.1029/2005JE002668

Sandwell, D. T. & MacKenzie, K. R. 1989. Geoid height versus topography for oceanic plateaus and swells. *Journal of Geophysical Research*, **94**, 7403–7418.

Schmalzl, J., Houseman, G. A. & Hansen, U. 1996. Mixing in vigorous time-dependent three-dimensional convection and application to earth's mantle. *Journal of Geophysical Research*, **101**, 21,847–21,858.

Schott, B., Van Den Berg, A. P. & Yuen, D. A. 2001. Focussed time-dependent Martian volcanism from chemical differentiation coupled with variable thermal conductivity. *Geophysical Research Letters*, **28**, 4271–4274.

Schubert, G., Solomon, S. C., Turcotte, D. L., Drake, M. J. & Sleep, N. H. 1990. Origin and thermal evolution of Mars. *In*: Kieffer, H., Jakosky, B., Snyder, C. & Matthews, M. (eds) *Mars*. University of Arizona Press, Tucson, AZ, 147–183.

Schultz, P. H., Schultz, R. A. & Rogers, J. 1982. The structure and evolution of ancient impact basins on Mars. *Journal of Geophysical Research*, **87**, 9803–9820.

Schwarz, S., Klugel, A. & Wohlgemuth-Ueberwasser, C. 2004. Melt extraction pathways and stagnation depths beneath the Madeira and Desertas rift zones (NE Atlantic) inferred from barometric studies. *Contributions to Mineralogy and Petrology*, **147**, 228–240.

Scoates, J. S., Cascio, M. L., Weis, D. & Lindsley, D. H. 2006. Experimental constraints on the origin and evolution of mildly alkalic basalts from the Kerguelen archipelago, southeast Indian Ocean. *Contributions to Mineralogy and Petrology*, **151**, 582–599.

Scott, E. D. & Wilson, L. 2000. Cyclical summit collapse events at Ascraeus Mons, Mars. *Journal of the Geological Society, London*, **157**, 1101–1106.

Silver, P. G., Russo, R. M. & Lithgow-Bertelloni, C. 1998. Coupling of South American and African plate motion and plate deformation. *Science*, **279**, 60–63.

Sleep, N. H. 1990. Hotspots and mantle plumes: some phenomenology. *Journal of Geophysical Research*, **95**, 6715–6736.

Sleep, N. H. 1994. Martian plate tectonics. *Journal of Geophysical Research*, **99**, 5639–5655.

Solomon, S. C. & Head, J. W. 1982. Evolution of the Tharsis province of Mars – the importance of heterogeneous lithospheric thickness and volcanic construction. *Journal of Geophysical Research*, **87**, 9755–9774.

Spohn, T., Grott, M. *et al.* 2012. INSIGHT: measuring the Martian heat flow using the heat flow and physical properties package (HP3). Paper 1445, presented at the 43rd Lunar and Planetary Science Conference, 19–23 March 2012, The Woodlands, TX.

Šrámek, O. & Zhong, S. 2012. Martian crustal dichotomy and Tharsis formation by partial melting coupled to early plume migration. *Journal of Geophysical Research – Planets*, **117**, E01005, http://dx.doi.org/10.1029/2011JE003867

Steinberger, B. & Antretter, M. 2006. Conduit diameter and buoyant rising speed of mantle plumes: implications for the motion of hot spots and shape of plume conduits. *Geochemistry, Geophysics, Geosystems*, **7**, Q11018, http://dx.doi.org/10.1029/2006GC001409

Stolper, E. M., Baker, M. B. *et al.* 2013. The petrochemistry of Jake-M: a Martian mugearite. *Science*, **341**, http://dx.doi.org/10.1126/science.1239463

Stroncik, N. A., Klugel, A. & Hansteen, T. H. 2009. The magmatic plumbing system beneath El Hierro (Canary Islands): constraints from phenocrysts and naturally quenched basaltic glasses in submarine rocks. *Contributions to Mineralogy and Petrology*, **157**, 593–607.

Taylor, G. J., Boynton, W. *et al.* 2006. Bulk composition and early differentiation of Mars. *Journal of Geophysical Research*, **111**, E3, http://dx.doi.org/10.1029/2005JE002645

Thomas, P. J., Squyres, S. W. & Carr, M. H. 1990. Flank tectonics of Martian volcanoes. *Journal of Geophysical Research*, **95**, 14,345–14,355.

Tosi, N., Plesa, A.-C. & Breuer, D. 2013. Overturn and evolution of a crystallized magma ocean: a numerical parameter study for Mars. *Journal of Geophysical Research*, **118**, 1–17, http://dx.doi.org/10.1002/jgre.20109

Wallace, P. J. 2002. Volatiles in submarine basaltic glasses from the Northern Kerguelen Plateau (ODP site 1140): implications for source region compositions, magmatic processes and plateau subsidence. *Journal of Petrology*, **43**, 1311–1326.

Watts, A. B., Pierce, C., Collier, J., Dalwood, R., Canales, J. P. & Henstock, T. J. 1997. A seismic study of Tenerife, Canary Islands: implications for volcano growth, lithospheric flexure and magmatic underplating. *Earth and Planetary Science Letters*, **146**, 431–447.

Wenzel, M. J., Manga, M. & Jellinek, A. M. 2004. Tharsis as a consequence of Mars' dichotomy and layered mantle. *Geophysical Research Letters*, **31**, 4, http://dx.doi.org/10.1029/2003GL019306

Werner, S. C. 2009. The global Martian volcanic evolutionary history. *Icarus*, **201**, 44–68.

Wilson, L. & Head, J. W. 1994. Mars-review and analysis of volcanic-eruption theory and relationships to observed landforms. *Reviews of Geophysics*, **32**, 221–263.

Wilson, L. & Head, J. W. 1998. Evolution of magma reservoirs within shield volcanoes on Mars. Abstract 1128, presented at the 29th Annual Lunar and Planetary Science Conference, 16–20 March 1998, Houston, TX.

Wilson, L., Scott, E. D. & Head, J. W. 2001. Evidence for episodicity in the magma supply to the large Tharsis volcanoes. *Journal of Geophysical Research*, **106**, 1423–1433.

Wilson, L., Mouginis-Mark, P. J., Tyson, S., Mackown, J. & Garbeil, H. 2009. Fissure eruptions in Tharsis, Mars: implications for eruption conditions and magma sources. *Journal of Volcanology and Geothermal Research*, **185**, 28–46.

Wilson, D. J., Peirce, C., Watts, A. B., Grevemeyer, I. & Krabbenhoeft, A. 2010. Uplift at lithospheric swells-I: seismic and gravity constraints on the crust and uppermost mantle structure of the Cape Verde mid-plate swell. *Geophysical Journal International*, **182**, 531–550.

Wise, D. U., Golombek, M. P. & McGill, G. E. 1979. Tectonic evolution of Mars. *Journal of Geophysical Research*, **84**, 7934–7939.

Yamamoto, M., Morgan, J. P. & Morgan, W. J. 2007. Global plume-fed asthenosphere flow-1: motivation and model development. *In*: Foulger, G. R. & Jurdy, D. M. (eds) *Plates, Plumes and Planetary Processes*. Geological Society of America Special Papers, **430**, 165–188.

Ye, S., Canales, J. P., Rhim, R., Danobeitia, J. J. & Gallart, J. 1999. A crustal transect through the northern and northeastern part of the volcanic edifice of Gran Canaria, Canary Islands. *Journal of Geodynamics*, **28**, 3–26.

Zhong, S. 2009. Migration of Tharsis volcanism on Mars caused by differential rotation of the lithosphere. *Nature Geoscience*, **2**, 19–23.

Zhong, S. J. & Zuber, M. T. 2001. Degree-1 mantle convection and the crustal dichotomy on Mars. *Earth and Planetary Science Letters*, **189**, 75–84.

Zuber, M. T. & Mouginis-Mark, P. J. 1992. Caldera subsidence and magma chamber depth of the Olympus Mons volcano. *Journal of Geophysical Research Letters*, **97**, 18 295–18 307.

Zuber, M. T., Solomon, S. C. *et al.* 2000. Internal structure and early thermal evolution of Mars from Mars Global Surveyor topography and gravity. *Science*, **287**, 1788–1793.